Evanescent microwave probes on high-resistivity silicon and its application in characterization of semiconductors

M. Tabib-Azar,[a] D. Akinwande, G. E. Ponchak,[b] and S. R. LeClair[c]
Electrical Engineering and Applied Physics, Case Western Reserve University, Cleveland, Ohio 44106

(Received 15 February 1999; accepted for publication 10 March 1999)

In this article we report the design, fabrication, and characterization of very high quality factor 10 GHz microstrip resonators on high-resistivity (high-ρ) silicon substrates. Our experiments show that an external quality factor of over 13 000 can be achieved on microstripline resonators on high-ρ silicon substrates. Such a high Q factor enables integration of arrays of previously reported evanescent microwave probe (EMP) on silicon cantilever beams. We also demonstrate that electron–hole pair recombination and generation lifetimes of silicon can be conveniently measured by illuminating the resonator using a pulsed light. Alternatively, the EMP was also used to nondestructively monitor excess carrier generation and recombination process in a semiconductor placed near the two-dimensional resonator. © *1999 American Institute of Physics.* [S0034-6748(99)00807-2]

I. INTRODUCTION

The development of high frequency resonators on silicon substrates has been limited by the performance degradation associated with common silicon at high frequencies. Since the resistivity of common grade silicon wafers is in the range of 1–20 Ω cm, circuit elements and transmission lines fabricated on it have high loss, resulting in low quality factors. alternative techniques have been developed to solve this problem. For example, one can use commercially available high resistivity silicon wafers ($\rho \approx 2500$ Ω cm). All of the circuit elements in this case may be implemented in the same way as they are implemented on GaAs, ceramic, or duroid substrates.

High resistivity (high-ρ) silicon wafers have been used to design and fabricate microstriplines,[1] coplanar wave guide and coplanar stripline transmission lines,[2,3] and antennas.[4–7] Even then the quality factor for resonators on high-ρ silicon[8] is only a few hundred. This article furthers the research in resonators on high-ρ silicon a step further by tuning the resonator to achieve an external quality factor[5] two orders of magnitude higher than the previously reported values.

We also describe an easy and convenient way of characterizing semiconductors by directly measuring their electron–hole pair generation and recombination lifetimes. With this information, one can further determine the concentration of free carriers.

The main objective of our work is to implement arrays of evanescent microwave probes (EMPs) on silicon cantilever beams with their own piezoelectric actuators. It has been demonstrated in the past that EMPs can be used to overcome the so-called Abbe barrier[9–15] in imaging nonuniformities in materials with a spatial resolution (≈ 0.4 μm at 1 GHz) much better than the wavelength ($\approx$30 cm at 1 GHz). Integrating EMPs on silicon is the first step toward designing and fabricating arrays of actuated EMPs for large area scanning and characterization of a variety of materials including metals, semiconductors, insulators, and biological specimens.

II. RESONATOR DESIGN

The end-coupled, half wavelength, $\lambda/2$, microstrip line on silicon, shown in Fig. 1, was designed to operate at 10 GHz using accepted equations from the literature.[6] The impedance was set to be 50 Ω in order to match other connectors and components used in the experimental setup. To achieve a high Q resonator, critical coupling between the feed line and the resonator is essential. Therefore, the key design parameter is the coupling capacitance, otherwise known as the coupling gap between the feed line and the resonator. However, there are no verified equations for the coupling gas as a function of material and design parameters in the literature. An empirical formula for the coupling gap that yields a moderate coupling is reported in Ref. 7. Using the results reported in Ref. 7, we estimated the gap dimension of 15–19 μm needed to achieve critical coupling in our microstripline (feed line length=17.55 mm, resonator length =5.4 mm, and microstripline width=0.3 mm). Then using the estimated value of the coupling gap we simulated and designed the microstripline using a finite element program (SONNET). We repeated this process until a satisfactory maximum reflection coefficient was obtained using SONNET at a gap dimension of 17 μm. Figure 2(a) shows the simulated reflection coefficient magnitude $|S_{11}|$ of the microstrip resonator. At the resonance frequency (9.5 GHz) the simulated $|S_{11}|$ magnitude was around -13.5 dB.

III. FABRICATION

The microstrip resonator was fabricated using the standard ''lift-off'' photolithography process. In the lift-off pro-

[a]Electronic mail: mxt7@po.cwru.edu
[b]Also with: NASA Lewis Research Center, Cleveland, OH 44135.
[c]Also with: Air Force Research Laboratory, Materials and Manufacturing Directorate, Wright-Patterson AFB, OH 45433.

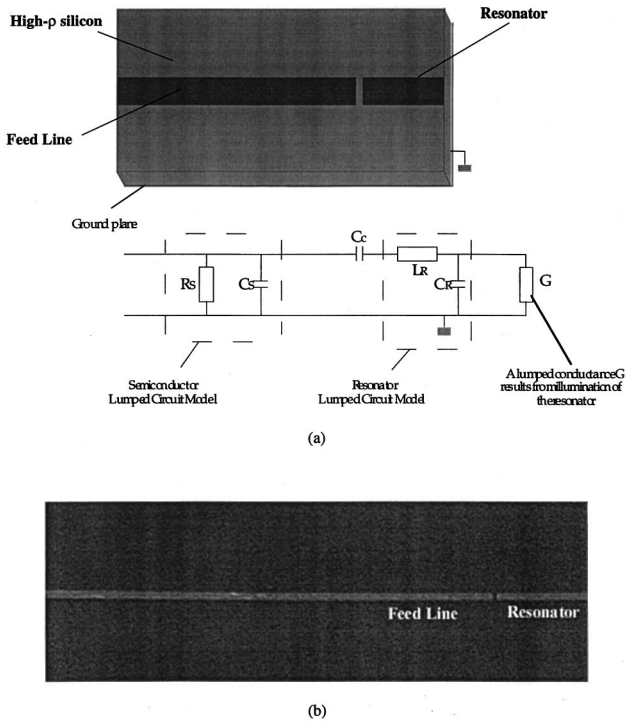

FIG. 1. Lumped circuit model of microstripline resonator on silicon and the actual image of the fabricated microstripline resonator on high-resistivity silicon substrate.

cess, a layer of positive photoresist is spin coated on the high resistivity silicon wafer at high speeds to obtain a uniform film. The wafer was then exposed to ultraviolet (UV) light through a negative patterned chromium–glass mask. The coated wafer is then soaked in chlorobenzene, which makes the top surface of the resist impervious to development. After development, a 0.2 μm layer of titanium is evaporated onto the entire surface to enhance adhesion followed by 1.5 μm of gold deposition. Finally, the resist is removed in acetone or a similar solvent.

IV. CHARACTERIZATION

The resonator was characterized under room conditions using a HP 8510C network analyzer. Figure 2(b) shows the measured reflection coefficient magnitude $|S_{11}|$ of the microstrip resonator, which agrees well with the simulated response. The slight discrepancy in the measured versus simulated results may be attributed to approximations made in simulating the resonator on silicon as a lossless ideal dielectric, and other approximations made by the software in its modified method of moments algorithm. This may also account for the nonzero capacitance and inductance at the resonant frequency.

To eliminate the unwanted capacitance and inductance, and compensate for coupling losses due to fringing fields,[7] the circuit was tuned by placing a dielectric ($\epsilon_r = 10.8$) on the coupling feedline of the resonator. This tuning resulted in a purely real 50 Ω impedance of the microstripline at resonance frequency [Fig. 3(a)]. The amount of dielectric used and the position on the strip occupied was determined by

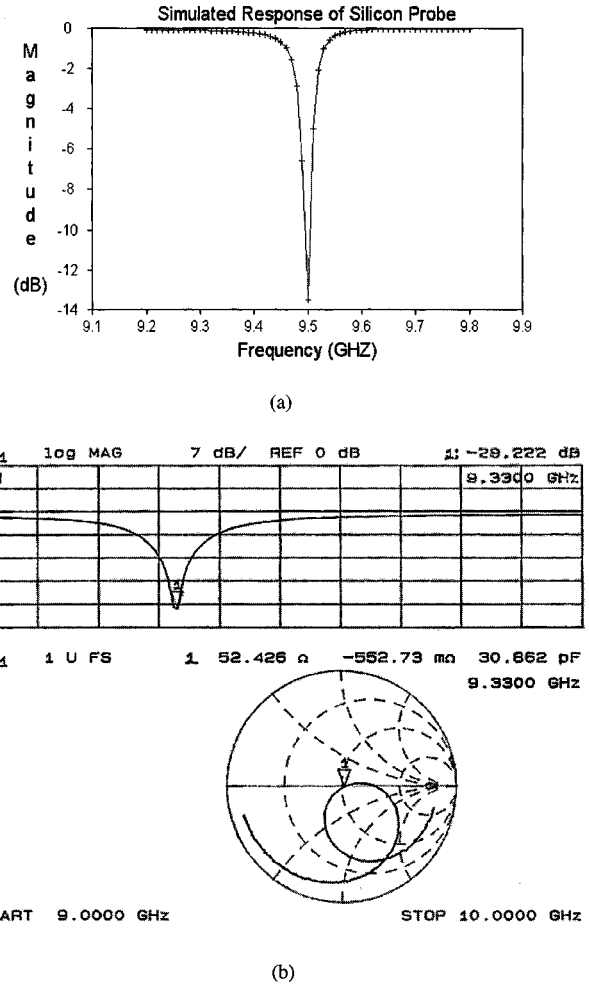

FIG. 2. (a) Simulated $|S_{11}|$ of microstripline resonator. (b) Measured untuned $|S_{11}|$ of microstripline resonator and viewed on a Smith Chart. The impedance at the resonance frequency was 50 Ω with negligible capacitance or inductance.

trial and error. The authors were able to achieve $|S_{11}|$ of -66 dB at resonance with an external quality factor of over 13 000 as shown in Fig. 3(b).

V. CARRIER LIFETIME MEASUREMENTS

The schematic of the experimental setup used to measure the carrier lifetimes is shown in Fig. 4. The resonator was coupled to a feed line that was fed by a 5.5–12.5 GHz signal generator through a circulator. A crystal microwave detector was connected to the circulator. The detector produced a dc voltage proportional to the magnitude of the reflected microwave. The detector output was directly monitored by an oscilloscope. The time response of the detector was faster than 0.1 μs and the oscilloscope had a bandwidth of 100 MHz. The microstripline was then illuminated by a pulsed xenon light source. To simplify the analysis presented next, we ensured that only the tip region of the microstripline resonator was illuminated. Thus, we can model the excess carrier region by a shunt resistor that connects the tip of the resonator to the ground plane.

The excess carriers that were generated by the switched illumination increased the conductivity of the high-ρ silicon

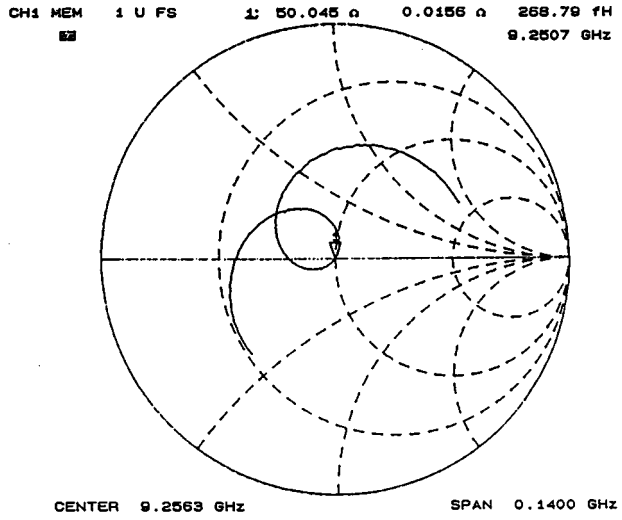

FIG. 3. (a) Measured tuned $|S_{11}|$ of microstripline resonator and viewed on a Smith Chart. (b) The tuned $|S_{11}|$ value was around -66 dB at resonance. The measured quality factor was over 13 000.

and resulted in a very lossy microstrip substrate. The microwave energy that was essentially stored in the resonator near the resonance frequency was then absorbed by the lossy illuminated substrate. When the illumination is turned off, it takes some time for the excess carriers to recombine. the recombination process could be monitored by monitoring the time evolution of the reflected microwave signal as can be seen in Fig. 5. The inverse process happens when the illumination is turned on. In this case the transient in the microwave signal reflects the excess carrier generation process. The turn-on time of the xenon lamp was very fast, on the order of a few nanoseconds, while its turn-off time was on the order of a few microseconds.

To relate the excess carrier lifetime to the reflection coefficient of the resonator, we note that the reflection coefficient is given by

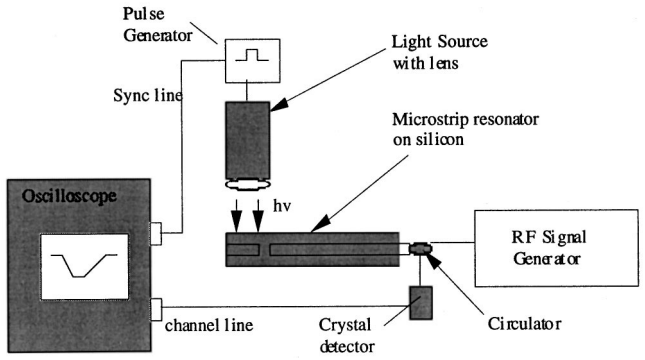

FIG. 4. Schematic of the experimental setup used in measuring the carrier lifetimes.

$$S_{11}=\frac{Z_{\text{total}}-Z_0}{Z_{\text{total}}+Z_0}, \tag{1}$$

where Z_0 is the characteristic impedance of the microstripline feed line and Z_{total} is the total impedance of the resonator. The relationship between S_{11} and free carrier concentration or photogenerated excess carriers can be quite involved a shown in Refs. 10 and 12. However, near resonance and in our highly tuned resonator $Z_{\text{total}}\approx Z_0$. Thus, we can write it as $Z_{\text{total}}=Z_0+\delta R_d$, where δR_d refers to the dark value of resistance. Under illumination, Z_{total} becomes $Z_0+\delta R_i$ where δR_i is the value of resistance under illumination. Thus, we can write the change in the reflection coefficient $[\Delta S_{11}(t)]$ as

$$\Delta S_{11}=\frac{G}{2Z_0\sigma_0}\frac{\delta n(t)}{n_0}, \tag{2}$$

where G is a geometry factor relating R to the conductivity, σ_0 is the dark conductivity of the silicon, n_0 is the thermal equilibrium electron concentration, and $\delta n(t)$ is the photogenerated excess carrier concentration. G may be affected by large area illumination of the microstripline. In our case, G is approximately fixed because we only illuminated the tip region of the microstripline resonator over a very small area. Thus, the only time dependent parameter in the above equation is the excess carrier concentration.

Moreover, it is well known that $\delta n(t)=\delta n(0)e^{-t/\tau}$, where $\delta n(0)$ is the steady-state value of the excess carrier concentration under constant illumination, and τ is the carrier

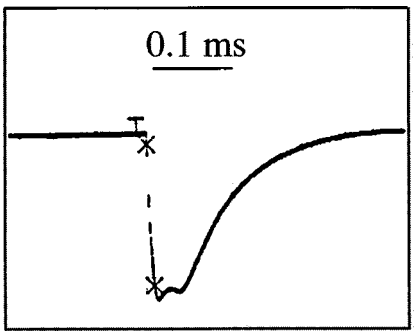

FIG. 5. The generation and recombination of excess carriers in high-resistivity silicon. The measured fall and rise times which correspond to the generation and recombination lifetimes, respectively, were 25 and 484 μs.

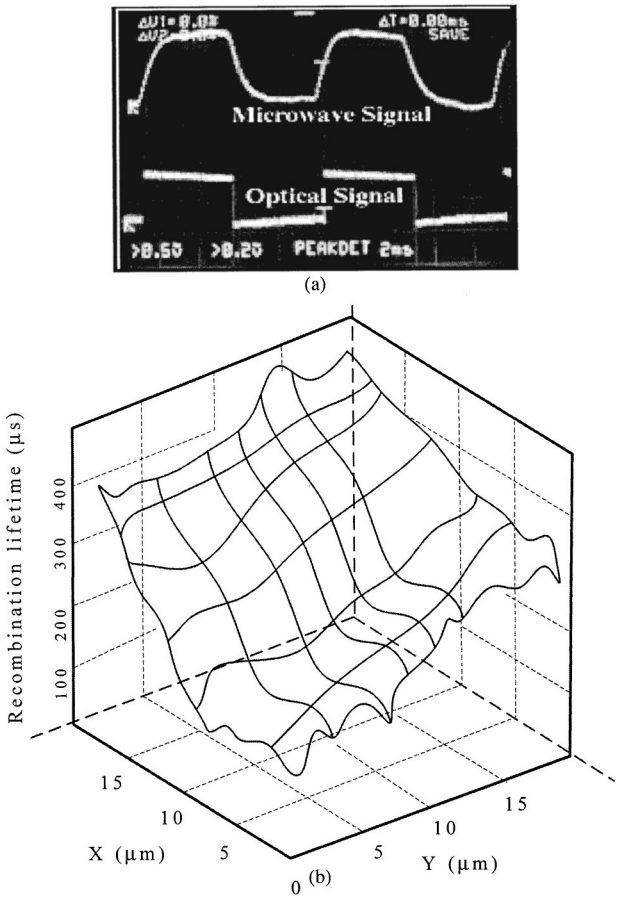

FIG. 6. Carrier lifetime measurement using the EMP. (a) The lower trace shows the optical pulse used to illuminate the semiconductor sample. The upper trace shows the EMP's response to the optical pulse. The carrier recombination lifetime is calculated from the transient behavior of EMP output when the optical pulse is turned off. (b) A carrier lifetime map over a silicon wafer that was nondestructively obtained by a scanning evanescent microwave probe while illuminating with a pulsed white light.

lifetime. Using Eq. (2) and Fig. 5, we calculated a carrier recombination lifetime of ≈ 484 μs. The carrier recombination lifetime reported for the high resistivity silicon substrate by the manufacturer was 500 μs.[8] The carrier recombination rate for our illumination was around $10^{19}\,\mathrm{cm}^{-3}\,\mathrm{s}^{-1}$, resulting in an excess carrier concentration $[\delta n(0)]$ of $2\times 10^{15}\,\mathrm{cm}^{-3}$ under steady-state illumination. From the fast apparent generation time constant of 25 μs in Fig. 5, one can be sure that the charging time of the microstripline resonator was not a limiting factor in determining the recombination lifetime.

In Fig. 6(b) we show the detection of photogenerated excess carriers in a silicon sample placed near a different EMP probe with a Duroid substrate. The EMP probe can nondestructively detect the conductivity of a semiconductor placed near its tip. Thus, it can be used to obtain a map of the carrier recombination lifetime across the sample as shown in Fig. 6(b). In this experiment the EMP was scanned over a silicon wafer as discussed in Refs. 10–15.

Since the microwave probe response is quite fast, an external stimulus, such as an optical pulse or a depleting high-power electromagnetic pulse, can be used to perturb the semiconductor's surface condition. Then, using the microwave probe one can monitor the recovery of the semiconductor surface after the perturbation is turned off. These transient measurements can be performed at different temperatures and since the microwave probe measurement is noncontact, only the semiconductor sample needs to be cooled or heated. Thus, activation energies and various parameters of deep levels, such as their capture/emission cross sections, and densities can be determined.

[1] W. Durr, U. Erben, A. Schuppen, H. Dietrich, and H. Schumacher, IEEE Trans. Microwave Theory Tech. **46**, 712 (1998).
[2] G. Ponchak and L. Katehi, IEEE Trans. Microwave Theory Tech. **45**, 970 (1997).
[3] R. Simons, S. Taub, and P. Young, Electron. Lett. **28**, 2209 (1992).
[4] R. Simons, S. Taub, and R. Lee, NASA Report No. TM-106057 (1993).
[5] A. Khanna and Y. Garault, IEEE Trans. Microwave Theory Tech. **MTT-31**, 261 (1983).
[6] R. E. Collins, *Foundations of Microwave Engineering* (McGraw-Hill, New York, 1966).
[7] R. Romanofsky, NASA Report No. TP-2899 (1989).
[8] Topsil Semiconductor Materials, Gilbert, AZ.
[9] E. A. Ash and G. Nicholls, Nature (London) **237**, 510 (1972).
[10] M. Tabib-Azar, N. Shoemaker, and S. Harris, Meas. Sci. Technol. **3**, 583 (1993).
[11] M. Tabib-Azar, D.-P. Su, A. Pohar, G. Ponchak, and S. R. LeClair, Rev. Sci. Instrum. **70**, 1725 (1999).
[12] M. Tabib-Azar, S. R. Leclair, and G. Ponchak, Rev. Sci. Instrum. (submitted).
[13] M. Tabib-Azar, S. L. LeClair, and G. Ponchak, IEEE MTT-S, Special Issue, Dec. (1999).
[14] R. Ciocan and M. Tabib-Azar, Rev. Sci. Instrum. (submitted).
[15] M. Tabib-Azar, P. S. Pathak, G. Ponchak, and S. R. LeClair, Rev. Sci. Instrum. **70**, 1 (1999).